Carnosic acid alleviates brain injury through NF-κB-regulated inflammation and Caspase-3-associated apoptosis in high fat-induced mouse models

YONG LIU*, YAN ZHANG*, MING HU, YU-HU LI and XING-HUA CAO

Department of Anesthesiology, Traditional Chinese Medicine Hospital Affiliated to Xinjiang Medical University, Urumqi, Xinjiang 830099, P.R. China

Received June 27, 2018; Accepted April 8, 2019

DOI: 10.3892/mmr.2019.10299

Abstract. High fat diet (HFD) is a risk factor for various diseases in humans and animals. Metabolic disease-induced brain injury is becoming an increasingly popular research topic. Carnosic acid (CA) is a phenolic diterpene synthesized by plants belonging to the Lamiaceae family, which exhibits multiple biological activities. In the present study, a mouse model of HFD-induced metabolic syndrome was generated. The body weight, liver weight, daily food intake, daily caloric intake, serum TG, serum TC, serum insulin and serum glucose of animals treated with CA were recorded. Additionally, the gene and protein expression levels of inflammatory cytokines, NF-κB signaling componnts, and caspase-3 were evaluated in the various CA treatment groups via immunohistochemical analysis, western blotting, reverse transcription-quantitative PCR. CA treatment significantly decreased HFD-induced metabolic syndrome by decreasing the serum levels of triglycerides, total cholesterol, insulin and glucose. Furthermore, CA served a protective role against brain injury by inhibiting the inflammatory response. CA significantly decreased the protein expression levels of various pro-inflammatory cytokines in serum and brain tissues, including interleukin (IL)-1β, IL-6 and tumor necrosis factor-α, regulated by the NF-κB signaling pathway. In addition, CA was revealed to promote the expression levels of anti-apoptotic Bcl-2, and to decrease the expression levels of pro-apoptotic Bax and matrix metallopeptidase 9. The present results suggested that CA was able to alleviate brain injury by modulating the inflammatory response and the apoptotic pathway. Administration of CA may represent a novel therapeutic strategy to treat metabolic disease-induced brain injury in the future.

Correspondence to: Dr Yan Zhang, Department of Anesthesiology, Traditional Chinese Medicine Hospital Affiliated to Xinjiang Medical University, Outpatient Building, 116 Huanghe Road, Shayibake, Urumqi, Xinjiang 830099, P.R. China
E-mail: zhangyan830099@163.com

*Contributed equally

Key words: carnosic acid, brain injury, NF-κB, Caspase-3, Bcl-2

Introduction

Neurodegeneration is defined as a progressive loss of structure and/or function of neurons that may lead to neuronal cell death (1). Neurodegenerative diseases, including amyotrophic lateral sclerosis, Parkinson's disease (PD), Alzheimer's disease (AD) and Huntington's disease, have been observed to be a result of neurodegenerative processes (2,3). Accumulating evidence has demonstrated the association between inflammatory responses and brain injury (3). In diseases associated with the central nervous system, the structure of the blood-brain barrier is frequently impaired; consequently, lymphocytes are able to enter the brain parenchyma through the blood-brain barrier (4). These immune cells may initiate various physiopathological reactions in the brain, and the activation of certain signaling pathways is able to mediate the elimination of various infectious agents (5). Metabolic disorders, including type II diabetes and obesity, are the principal factors associated with metabolic inflammation (6). A previous study identified that metabolic diseases may mediate the association between neurodegeneration and brain injury (7). Previous studies have identified that the inflammatory response is associated with various neurodegenerative pathways (8). Furthermore, pro-inflammatory cytokines, including tumor necrosis factor (TNF)-α, interleukin (IL)-1β and IL-6, have been reported to serve important roles in the pathophysiology of depression (9,10). The release of inflammatory cytokines is primarily regulated by the NF-κB signaling pathway; therefore, the NF-κB signaling pathway may be involved in the brain injury response (11). Apoptotic cell death, mediated by Caspase-3, has been identified to be associated with brain injury; this apoptotic pathway is associated with multiple pro-apoptotic and anti-apoptotic factors, including Bcl-2, Bax and matrix metallopeptidase 9 (MMP-9) (12-14). However, the role of these pathways in metabolic diseases and brain injury remains unclear. Therefore, it is necessary to understand the molecular mechanisms underlying the associations among metabolic disorders, inflammatory response and brain injury. The present study aimed to examine the roles of the NF-κB and

Caspase-3 signaling pathways in the process of brain injury in high fat-induced mouse models.

Carnosic acid (CA) is a benzenediol abietane diterpene extracted from rosemary and common sage. A previous study demonstrated that CA may be used as a preservative and anti-oxidant in various products, including toothpaste, mouthwash and chewing gum (15). In addition, CA has been reported to exhibit anti-tumor effects on colon cancer, breast cancer and skin tumor (16). CA may affect multiple biological processes, including cell growth, cell apoptosis, reactive oxygen species (ROS) release and inflammatory response (17). CA has also been demonstrated to be associated with ROS, which can regulate the expression levels of antioxidant phase II enzymes, including nicotinamide-adenine dinucleotide phosphate quinone dehydrogenase 1, glutathione-S-transferase and uridine diphosphate glucuronosyltransferase (18). Therefore, CA may be able to increase the antioxidant ability of cells and organisms.

CA is able to regulate the inflammatory response by decreasing the expression levels of inflammatory mediators, including TNF-α (19). In addition, CA may inhibit activation of the NF-κB signaling pathway by increasing the activity or the expression levels of various molecular components including spleen-associated tyrosine kinase, SRC proto-oncogene, non-receptor tyrosine kinase, PI3K, pyruvate dehydrogenase kinase 1, Akt, IκB kinase (IKK) and NF-κB inhibitor α (IκBα) (20). In addition, CA serves important roles in neuroprotection. CA has been identified to inhibit the synthesis of amyloid-β 1-42 in SH-SY5Y cells by increasing the expression levels of the p53-dependent metalloproteinase ADAM metallopeptidase domain 17 (21). In addition, CA is able to increase the synthesis of glutathione, and to repress the JNK and p38 signaling pathways, via the nuclear factor, erythroid 2 like 2 pathway, which may inhibit 6-hydroxydopamine-induced apoptosis of SH-SY5Y cells (22). These effects suggest that administration of CA may represent a novel therapeutic strategy to treat AD and PD. Since CA has been identified to exhibit anti-inflammatory and anti-apoptotic functions in cancer cells, the present study aimed to determine whether treatment with CA is able to mediate the inflammatory response following injury, thus facilitating the repair of the damaged tissue.

In the present study, mice fed a high-fat diet (HFD) were used to establish animal models of brain injury, and the effects of CA were investigated. Furthermore, the mRNA and protein expression levels of factors involved in the NF-κB and Caspase-3 signaling pathways were examined.

Materials and methods

Animals. All animals were treated according to the guidelines for the Care and Use of Laboratory Animals (23), and the study was approved by The Committee on The Ethics of Animal Experiments of Xinjiang Medical University (approval no. XM2017MD). In total, 40 male C57BL/6 mice (weight, 18-22 g; age, 6 weeks) were purchased from The Experimental Animal Center of Nanjing Medical University (certificate of conformity no. SCXK JS 2016-0002). Mice were acclimatized for 7 days prior to the start of the study. Mice were provided access to drinking water and standard rodent chow *ad libitum*. The temperature of housing environment was set as 22±2˚C. The relative humidity was set at 60±10% under a 12-h light/dark cycle. The mice were randomly divided into four groups: i) Control mice (Con); ii) HFD mice (Veh); iii) HFD mice treated with 10 mg/kg CA (CA-L); and iv) HFD mice treated with 20 mg/kg CA (CA-H). The HFD protocol was performed according to a previous study (24). CA was purchased from Changsha Yaying Biotechnology Co., Ltd. CA solution was prepared according to a previous study (18). Mice were treated with CA via gavage for 9 weeks following a 6-week period of HFD. The caloric intake was calculated by subtracting the fecal caloric excretion (fecal caloric content x fecal excretion) from the dietary caloric intake (diet caloric content x food intake). After 15 weeks, all mice were fasted for 12 h. The blood of anesthetized mice was collected via retro-orbital puncture. Subsequently, body and liver weights were measured, and the brain, pancreas and whole liver tissues were collected at 4˚C. The tissues were frozen in liquid nitrogen and stored at -80˚C. For histology, the tissues were fixed in 10% neutral buffered formalin (saturated aqueous formaldehyde from Thermo Fisher Scientific, Inc., buffered to pH 6.8-7.2 with 100 mM phosphate buffer) for 24 h at 25˚C.

Biochemical analysis. According to the metabolic syndrome diagnostic criteria provided by the World Health Organization (25), insulin resistance (IR) is required to diagnose metabolic syndrome. In addition, to diagnose metabolic syndrome, two other criteria among the following five are required: Obesity (waist/hip ratio: >0.90 for males, >0.85 for females; or body mass index >30 kg/m^2), hyperglycemia, dyslipidemia [triglycerides (TG): >150 mg/dl or high-density lipoprotein cholesterol: <35 mg/dl for males, <39 mg/dl for females], hypertension (≥140/90 mmHg) and microalbuminuria. In the present study, IR, TG and hyperglycemia were selected to assess metabolic syndrome in mouse models. After 15 weeks, blood was collected by retro-orbital puncture method. Additionally, the serum was obtained from blood samples via centrifugation with 2,000 RPM (800 x g) for 15 min at 4˚C. Then, the serum was transferred to a 5-ml centrifuge tube, which was placed on the glacial table. Serum levels of TG (cat. no. A110-2-1) and total cholesterol (TC; cat. no. A111-2-1) were tested with biochemical kits (Nanjing Jiancheng Taihao Biotechnology Co., Ltd.). Glucose (cat. no. F006-1-1) and insulin (cat. no. H203) levels were also measured using biochemical kits (Nanjing Jiancheng Taihao Biotechnology Co., Ltd.).

ELISA measurement. After 15 weeks, the serum was obtained via centrifugation of blood samples with 2,000 RPM (800 x g) for 15 min at 4˚C. ELISA kits, including TNF-α (cat. no. MTA00B), IL-1β (cat. no. MLB00C) and IL-6 (cat. no. D6050) was used to identify the serum concentrations of these inflammatory cytokines. The detailed steps were followed according to the manufacturer's protocols (R&D System, Inc.). The standard curve for each cytokine was calculated; the concentration of the antigens was determined at 450 nm.

Histopathological examination. Histopathological evaluation was performed on the liver, pancreas and brain tissues of mice. Samples were fixed with 10% formalin buffer for 24 h at 25˚C. Subsequently, the pretreated samples were embedded

in paraffin and sliced (3-5 μm). H&E staining was performed according to the previous method (26). Briefly, samples were stained with hematoxylin for 10 min and with eosin for 1 min (both at room temperature) to establish the diagnosis areas. After H&E staining, histopathological alterations were observed using a light microscope. For each sample, three randomly selected microscopic fields of view were used to calculate the pathological scores. The microscopic fields were scored blindly using a scale from 0 (normal) to 5 (highly destructive pathology). The mean of the three values was used to calculate an overall pathological score, as previously described (27).

Additionally, immunohistochemical staining was performed on 3-5-μm thick paraffin-embedded tissue sections. Sections were deparaffinized in xylene, hydrated using a graded alcohol series, and washed with TBS for 10 min and distilled water for a further 10 min. Endogenous peroxidase activity was blocked with 3% v/v H_2O_2 in water for 5 min. Antigen retrieval was performed for all antibodies by placement of the sections in citrate buffer and heating in a microwave oven for 15 min. Sections were treated with 25 ml blocking buffer for 1 h at room temperature. The treated sections were separately incubated with primary antibodies for TNF-α (1:200; cat. no. 11948) and IL-1β (1:400; cat. no. 12703) at 4˚C overnight (both Cell Signaling Technology, Inc.). Then, all treated sections were incubated with the biotin-conjugated secondary antibody (1:800; cat. no. ab6720; Abcam) for 30 min at room temperature. The standard streptavidin-biotin-peroxidase complex method was performed using an LSAB System Universal kit (Dako; Agilent Technologies, Inc.) for 10 min, 3,3'-diaminobenzidine solution was used as a chromogen for 5 min, and all sections were counterstained with Mayer's haematoxylin for 1 min and mounted; all reactions were performed at room temperature. The species were observed under a light microscope (Eclipse 80i; Nikon Corporation). The percentage of IL-1β- and TNF-α-positive cells was calculated using the inForm cell analysis software (version 2.0.4743.16069; PerkinElmer, Inc.). The histopathological examination method was performed as previously described (28).

Western blot analysis. Total protein from different groups was extracted using the T-PER Tissue Protein Extraction Reagent kit (Thermo Fisher Scientific, Inc.). Protein concentration was determined using a bicinchoninic protein assay kit (Thermo Fisher Scientific, Inc.). Proteins (50 μg/lane) were separated by 10% SDS-PAGE. Subsequently, proteins were transferred to PVDF membranes, which were blocked with TBS containing 0.05% Tween-20 (TBS-T), supplemented with 5% skim milk (Sigma-Aldrich; Merck KGaA) at room temperature for 2 h on a rotating shaker. Membranes were subsequently washed with TBS-T. The primary antibodies used were as follows: IL-1β (1:100; cat. no. PA1351; Boster Biological Technology), IL-18 (1:500; cat. no. RP1017; Boster Biological Technology), TNF-α (1:500; cat. no. RP1000; Boster Biological Technology), IKKα (1:1,000; cat. no. 11930; Cell Signaling Technology, Inc.) and phosphorylated (p)-IKKα (1:1,000; cat. no. 2697; Cell Signaling Technology, Inc.), IκBα (1:500; cat. no. 4814; Cell Signaling Technology, Inc.) and p-IκBα (1:500; cat. no. 9246; Cell Signaling Technology, Inc.), NF-κB (1:1,000; cat. no. 8242; Cell Signaling Technology, Inc.) and p-NF-κB (1:1,000; cat. no. 3033; Cell Signaling Technology, Inc.), glial fibrillary acidic protein (GFAP; 1:2,000; cat. no. 3670; Cell Signaling Technology, Inc.), neuronal nuclei (Neu-N; 1:1,500; cat. no. 24307; Cell Signaling Technology, Inc.), ionized calcium-binding adapter molecule 1 (Iba-1; 1:2,000; cat. no. ab15690; Abcam), Bax (1:1,000; cat. no. ab32503; Abcam), Bcl-2 (1:1,500; cat. no. ab182858; Abcam), MMP-9 (1:100; cat. no. AF909; R&D Systems), Caspase-3 (1:400; cat. no. ab13585; Abcam), and GAPDH (1:1,000; cat. no. ab8245; Abcam). The antibodies were diluted in TBS-T and were incubated with the membranes at 4˚C overnight. Subsequently, the membranes were washed with TBS-T followed by incubation with ImmPRESS® HRP Universal Antibody Polymer Detection Kit (1:2,000; cat. no. MP-7500-15; Maravai LifeSciences) for 1 h at room temperature. The protein bands were detected using an ECL western blot detection kit (Thermo Fisher Scientific, Inc.). Western blot bands were observed with an ECL Western Blotting Analysis system (cat. no. RPN2108; GE Healthcare Life Sciences) and exposed to X-ray films (Kodak). Image Studio Lite Western Blot Analysis Software version 3.1 (LI-COR Biosciences) was chosen to perform pixel quantification of the images.

Reverse transcription-quantitative PCR (RT-qPCR) analysis. Total RNA was isolated from individual mouse brains using TRIzol® reagent (Invitrogen; Thermo Fisher Scientific, Inc.). The total RNA was used to evaluate the relative mRNA expression levels of IL-1β, IL-18, TNF-α, Bax, Bcl-2, MMP-9, Caspase-3 and GAPDH. The reverse transcribed cDNA was synthesized using the SuperScript First-Strand Synthesis kit (Invitrogen; Thermo Fisher Scientific, Inc.) according to the manufacturer's protocol. The primers used for qPCR are listed in Table I. Primer sequences were verified with NCBI primer blast tool to avoid non-specific annealing (https://www.ncbi.nlm.nih.gov/tools/primer-blast/). All primers were obtained from Sangon Biotech Co., Ltd. Reactions were performed in a total volume of 20 μl, and consisted of 10 μl 2X SYBR Green PCR master mix (cat. no. 4309155; Applied Biosystems; Thermo Fisher Scientific, Inc.), 1 μl forward primer (10 pmol), 1 μl reverse primer (10 pmol), 1 μl cDNA template and 7 μl double distilled water. The thermocycling conditions were as follows: 94˚C for 3 min, then 40 cycles of 95˚C for 15 sec and 60˚C for 25 sec. BioRad iCycler iQ detection system was used in this study (Bio-Rad Laboratories, Inc.). GAPDH was used as the reference gene. Normalization and fold change for each gene were calculated using the $2^{-\Delta\Delta Cq}$ method (29).

Statistical analysis. All experiments were repeated three times. Data are presented as the means ± SEM. Treated cells, tissues and the corresponding controls were compared using GraphPad Prism (version 6.0; GraphPad Software, Inc.). Multiple groups were compared using one-way ANOVA. Differences between groups were calculated using the Student-Newman-Keuls post hoc test. $P<0.05$ was considered to indicate a statistically significant difference.

Results

The effects of CA on metabolic syndrome. Metabolic disease has previously been reported to be associated with

Table I. Primers used in the reverse transcription-quantitative PCR analysis.

Gene symbol	Primer sequences (5'→3')
GAPDH	F: CATTCAAGACCGGACAGAGG
	R: ACATACTCAGCACCAGCATCACC
IL-6	F: GAACCGGCACCTGACACC
	R: CACGACTTCGTCACCGGTAA
TNF-α	F: AGCACAAAGAGAGTGTCGC
	R: AGTCGTCCAGTGTGTGTA
IL-1β	F: GAGTGATAGACAGCAAGCC
	R: GGCCGTCAATGTATGTTGGTG
IL-18	F: GCAGCAGGTGAGTGGGCAGT
	R: ACTGTCGCCTGGTTCTCTGTGC
Bax	F: CAGTTAGGAGACGACAG
	R: AGCGTCGCTGGATGTGTGA
MMP-9	F: CACCTTCTTGTCGACCGCCTA
	R: TCCGCGTCTGTTCGGCAT
Bcl-2	F: TCCTGGGACTCTTCTTATTTACCA
	R: TTGCCTGCTAAAGGCAATTACC
Caspase-3	F: GAGCAAGCAAGATTTACTCGA
	R: AGCCAGCTACATGGATCTAAA

IL, interleukin; TNF-α, tumor necrosis factor-α; MMP-9, matrix metallopeptidase 9.

neurodegenerative disease via the inflammatory response (30). A previous study suggested that HFD could induce metabolic diseases in rodents, causing type II diabetes characterized by IR (31). In the present study, animal models of metabolic syndrome were established by feeding mice a HFD. Mouse body weight in the Veh group was significantly higher than in the Con group (Fig. 1A; P<0.01). Conversely, high concentrations of CA could significantly reduce body weight compared with the Veh group (P<0.05). The present results suggested that CA induced body weight loss in a dose-dependent manner. Similarly, the liver weight in different groups was also measured. Liver weight increased significantly in the Veh group compared with in the Con group (P<0.05). Moreover, high CA was sufficient to significantly reduce the liver weight compared with the Veh group (P<0.05). The present results suggested that CA induced liver weight loss in a dose-dependent manner (Fig. 1B). In addition, the daily food intake in the Veh group was significantly lower than in the Con group (P<0.05). However, the daily food intake in the Veh group was restored following treatment with a high dosage of CA (P<0.05; Fig. 1C). Moreover, the daily caloric intake in the Veh group was significantly higher compared with that in the Con group (P<0.01). This effect was reversed by CA treatment (P<0.05; Fig. 1D). In addition, serum levels of TG, TC and insulin were analyzed. The present results suggested that TG, TC and insulin in the Veh group were significantly higher than in the Con group (P<0.001; Fig. 1E-G). Notably, CA treatment was able to significantly decrease the serum levels of TG, TC and insulin. In addition, the serum glucose level in the Veh group was significantly higher than the Con group (P<0.01). By contrast, serum glucose level was decreased following CA administration (Fig. 1H). The present results suggested that HFD could induce metabolic syndrome in mice, and the effects of HFD were reversed by CA administration. The present results indicated that CA may be used to treat metabolic syndrome.

CA reduces the inflammatory response. In order to investigate whether CA could improve metabolic disease-associated inflammatory response, the relative expression levels of key factors associated with the inflammatory response were examined. HFD induced the inflammatory response in mouse liver tissue (Fig. 2A). The pathological score in the Veh group (pathological score, 3.2) was significantly higher than the Con group (pathological score, 0; P<0.001). By contrast, mice in the CA-L and CA-H groups exhibited a significant decrease in the pathological score (pathological scores, 1 and 0.8, respectively) compared with the Veh group (pathological score, 3.2; P<0.01). Moreover, pancreas injury was observed in the Veh group (Fig. 2B; pathological score, 3.0). Pancreas injury was significantly decreased following CA administration (pathological scores, 0.8 and 0.5 in the CA-L and CA-H groups, respectively). TNF-α and IL-1β are important pro-inflammatory cytokines, with a role in various diseases (32). Immunohistochemistry was performed to investigate the protein expression levels of TNF-α and IL-1β in mouse livers (Fig. 2C and D). The protein expression levels of TNF-α and IL-1β were significantly upregulated in the Veh group compared with in the Con group (P<0.001). Treatment with CA was able to significantly decrease the expression levels of both factors (P<0.001). The present results suggested that CA effectively inhibited the inflammatory response. Moreover, the serum levels of pro-inflammatory cytokines, including IL-1β, IL-6 and TNF-α, were investigated. The concentrations of IL-1β, IL-6 and TNF-α in the Veh group were significantly higher than in the Con group (P<0.001). The concentrations of these three pro-inflammatory cytokines were significantly reduced following treatment with CA (Fig. 2E-G). Collectively, the present results suggested that HFD promoted metabolism-associated inflammatory response in mice, and treatment with CA effectively inhibited the secretion of pro-inflammatory cytokines in mice fed a HFD.

CA regulates the secretion of pro-inflammatory cytokines in the brain. Central nervous system injury caused by metabolic disease has been previously described (33). However, to the best of our knowledge, no effective therapeutic strategies are currently available. In the present study, brain injury was observed following HFD, as indicated by high protein expression levels of TNF-α and IL-1β in the brain (Fig. 3A). The present results suggested that HFD induced metabolic syndrome and brain injury in mice. Additionally, CA was able to inhibit the expression levels of TNF-α and IL-1β. Western blot analysis was performed to examine the protein expression levels of mature IL-1β and IL-18 in mouse brain tissues following different treatments. The protein expression levels of mature IL-1β and IL-18 were significantly higher in the Veh group compared with in the Con group (P<0.001). CA treatment decreased the protein expression levels of mature IL-1β and IL-18 compared with in the Veh group (P<0.001;

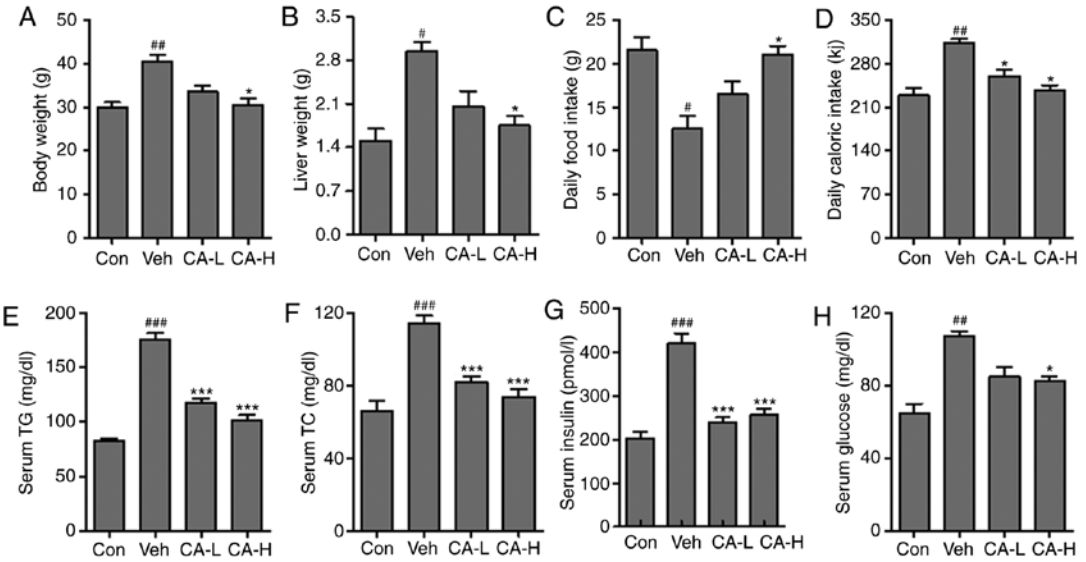

Figure 1. Effects of CA on metabolic syndrome in HFD mice. (A) Body weight, (B) liver weight, (C) daily food intake and (D) daily caloric intake measured in the four experimental groups. Serum levels of (E) TG, (F) TC, (G) insulin and (H) glucose. Data are expressed as the means ± SEM. N=10/group. $^{\#}$P<0.05, $^{\#\#}$P<0.01 and $^{\#\#\#}$P<0.001 vs. Con; *P<0.05 and ***P<0.001 vs. Veh. CA, carnosic acid; CA-H, HFD mice treated with 20 mg/kg CA; CA-L, HFD mice treated with 10 mg/kg CA; Con, Control group; HFD, high-fat diet; TC, total cholesterol; TG, triglycerides; Veh, HFD mice.

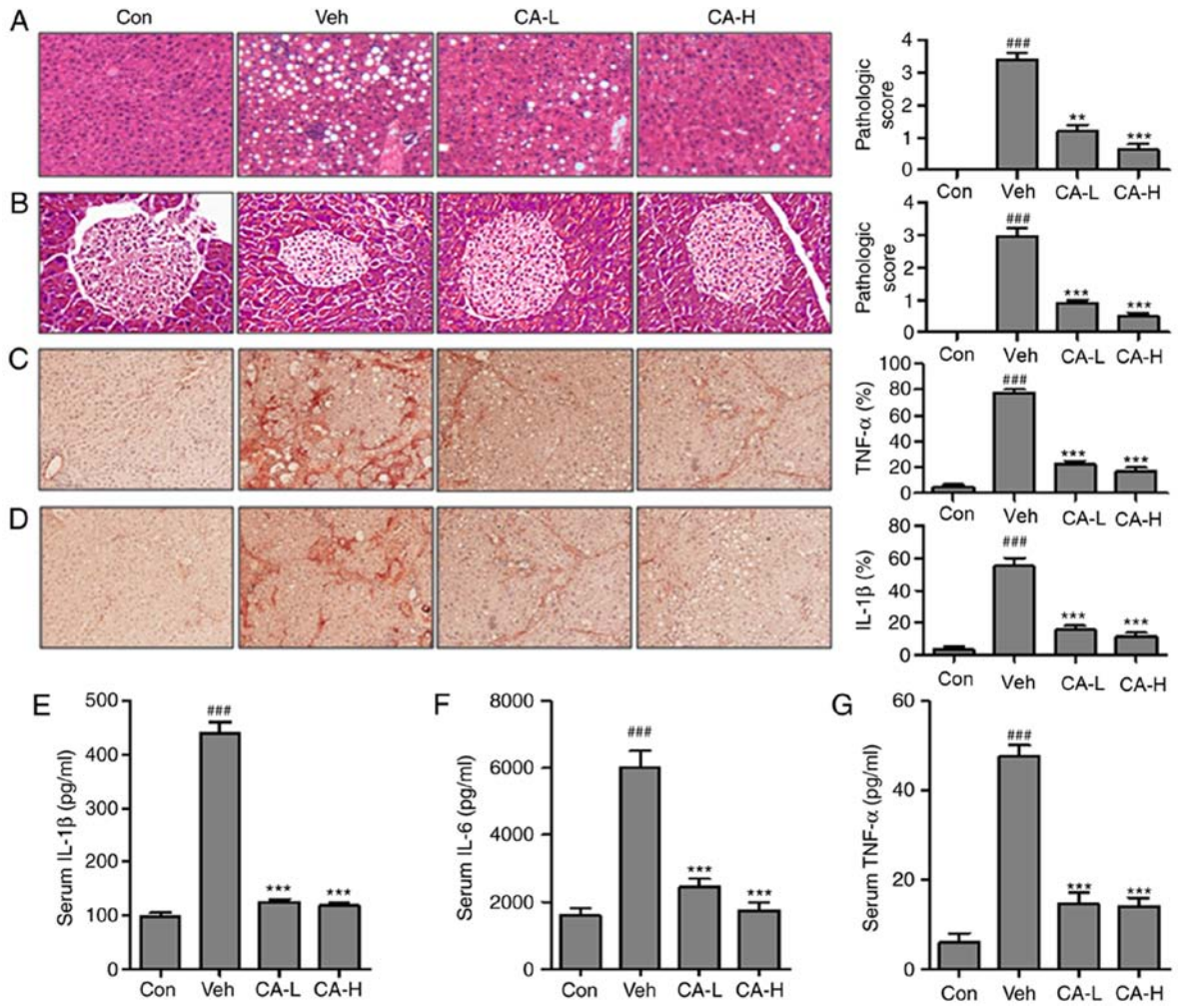

Figure 2. CA decreases the inflammatory response in HFD mice. Hematoxylin and eosin staining of (A) liver and (B) pancreas indicated the pathological score in different experimental groups (magnification, x50). Immunohistochemical analysis of (C) TNF-α and (D) IL-1β in the liver of HFD mice and percentage of positive cells. Serum levels of (E) IL-1β, (F) IL-6 and (G) TNF-α. Data are expressed as the means ± SEM. n=10 in each group. $^{\#\#\#}$P<0.001 vs. Con; **P<0.01 and ***P<0.001 vs. Veh. CA, carnosic acid; CA-H, HFD mice treated with 20 mg/kg CA; CA-L, HFD mice treated with 10 mg/kg CA; Con, Control group; HFD, high-fat diet; IL, interleukin; TNF-α, tumor necrosis factor-α; Veh, HFD mice.

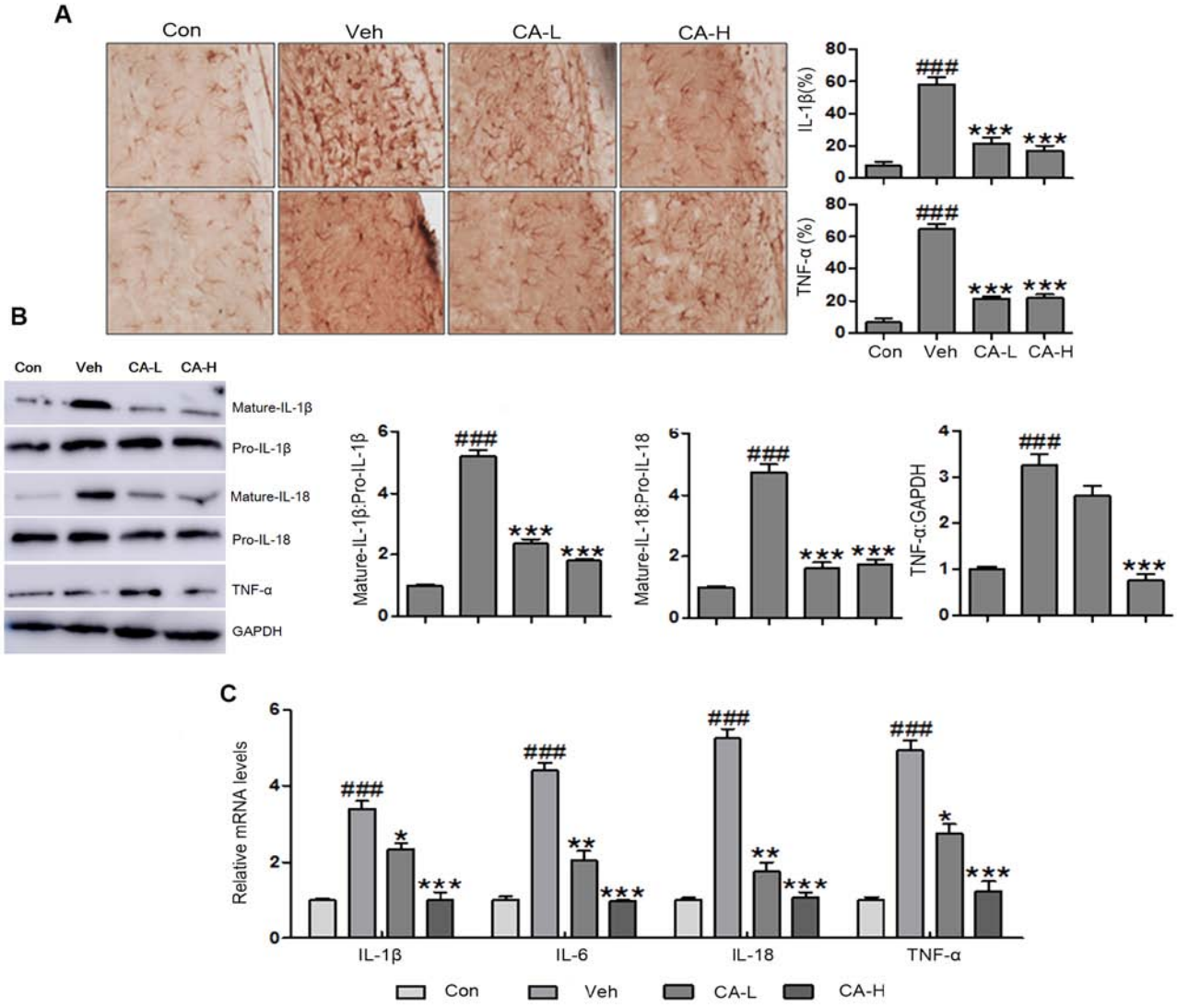

Figure 3. Effects of CA on the secretion of pro-inflammatory cytokines in the brain of HFD mice. (A) Immunohistochemical analysis of IL-1β and TNF-α in brain tissues of HFD mice (magnification, x50). (B) Protein expression levels of IL-1β, IL-18 and TNF-α in HFD mice, as assessed by western blot analysis. (C) mRNA expression levels of pro-inflammatory cytokines in the brain of HFD mice, as assessed by reverse transcription-quantitative PCR analysis. Data are expressed as the means ± SEM. n=10 in each group. $^{###}$P<0.001 vs. Con; *P<0.05, **P<0.01 and ***P<0.001 vs. Veh. CA, carnosic acid; CA-H, HFD mice treated with 20 mg/kg CA; CA-L, HFD mice treated with 10 mg/kg CA; Con, Control group; HFD, high-fat diet; IL, interleukin; TNF-α, tumor necrosis factor-α; Veh, HFD mice.

Fig. 3B and C). Furthermore, the protein expression levels of TNF-α were upregulated in brain tissue collected from Veh mice (P<0.001). Notably, the protein expression levels of TNF-α were reduced following CA administration (P<0.001; Fig. 3B). In addition, RT-qPCR was used to investigate the mRNA expression levels of pro-inflammatory cytokines, including IL-1β, IL-6, IL-18 and TNF-α. The present results suggested that IL-1β, IL-6, IL-18 and TNF-α were upregulated in the Veh group compared with in the Con group (P<0.001). Notably, the expression levels of these genes were reduced following CA administration (P<0.001). The present qPCR results were consistent with the aforementioned western blotting results (Fig. 3C). Collectively, the present results suggested that CA inhibited the secretion of inflammatory cytokines in a mouse model of brain injury induced by HFD.

CA improves brain injury by suppressing the NF-κB signaling pathway. The NF-κB signaling pathway has been reported to be associated with the secretion of pro-inflammatory cytokines (34). The protein expression levels of p-IKKα, p-IκBα and p-NF-κB in the Veh group were increased compared with in the Con group (P<0.01; Fig. 4A). Notably, the protein expression levels of p-IKKα, p-IκBα and p-NF-κB were significantly reduced following CA administration (P<0.05). The present results suggested that brain injury caused by HFD involved the NF-κB signaling pathway, and CA was a negative regulator of the NF-κB signaling pathway. As a biomarker of nerve injury, GFAP is expressed in astrocytes (35). In the present study, GFAP was highly expressed in mouse brain tissues. High CA dosage decreased the expression levels of GFAP (Fig. 4A). However, low CA dosage did not affect the protein expression levels of GFAP. The present data suggested that CA influenced the expression levels of GFAP in a dose-dependent manner. Additionally, the protein expression levels of Neu-N and Iba1 were decreased following treatment with CA at low and high concentrations (Fig. 4B and C). Notably, the protein expression

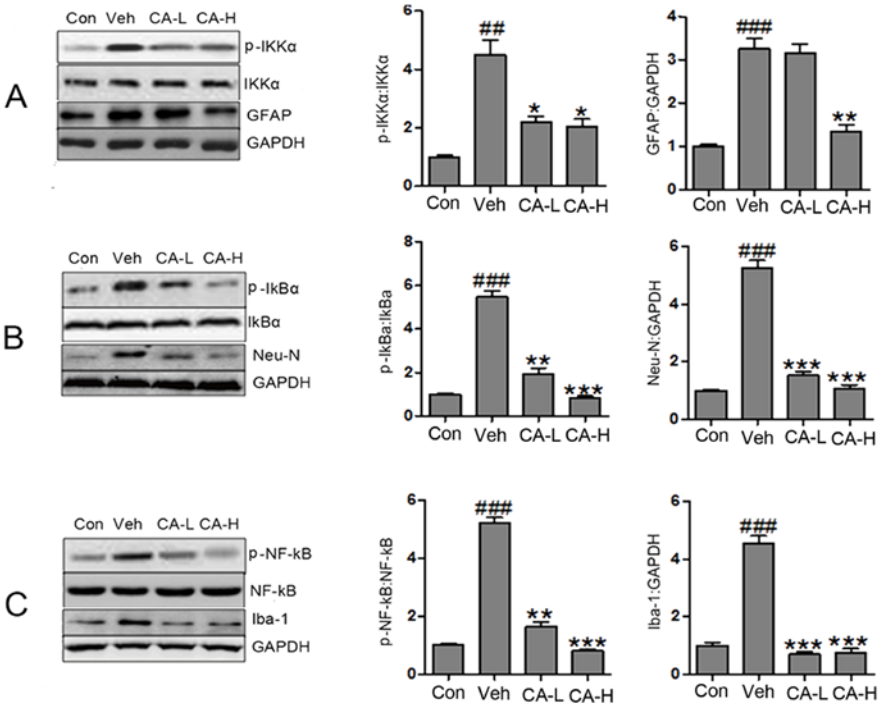

Figure 4. CA attenuates brain injury in HFD mice by inactivating the NF-κB signaling pathway. (A) Protein expression levels of p-IKKα, IKKα, GFAP and GAPDH in different groups, as assessed by western blot analysis. (B) Protein expression levels of p-IκBα, IκBα, Neu-N and GAPDH in different groups, as assessed by western blot analysis. (C) Protein expression levels of p-NF-κB, NF-κB, Iba-1 and GAPDH in different groups, as assessed by western blot analysis. Data are expressed as the means ± SEM. n=10 in each group. $^{\#\#}$P<0.01 and $^{\#\#\#}$P<0.001 vs. Con; *P<0.05, **P<0.01 and ***P<0.001 vs. Veh. CA, carnosic acid; CA-H, HFD mice treated with 20 mg/kg CA; CA-L, HFD mice treated with 10 mg/kg CA; Con, Control group; GFAP, glial fibrillary acidic protein; HFD, high-fat diet; IκBα, NF-κB inhibitor α; IKKα, IκB kinase α; Neu-N, neuronal nuclei; Iba-1, ionized calcium-binding adapter molecule 1; p, phosphorylated; Veh, HFD mice.

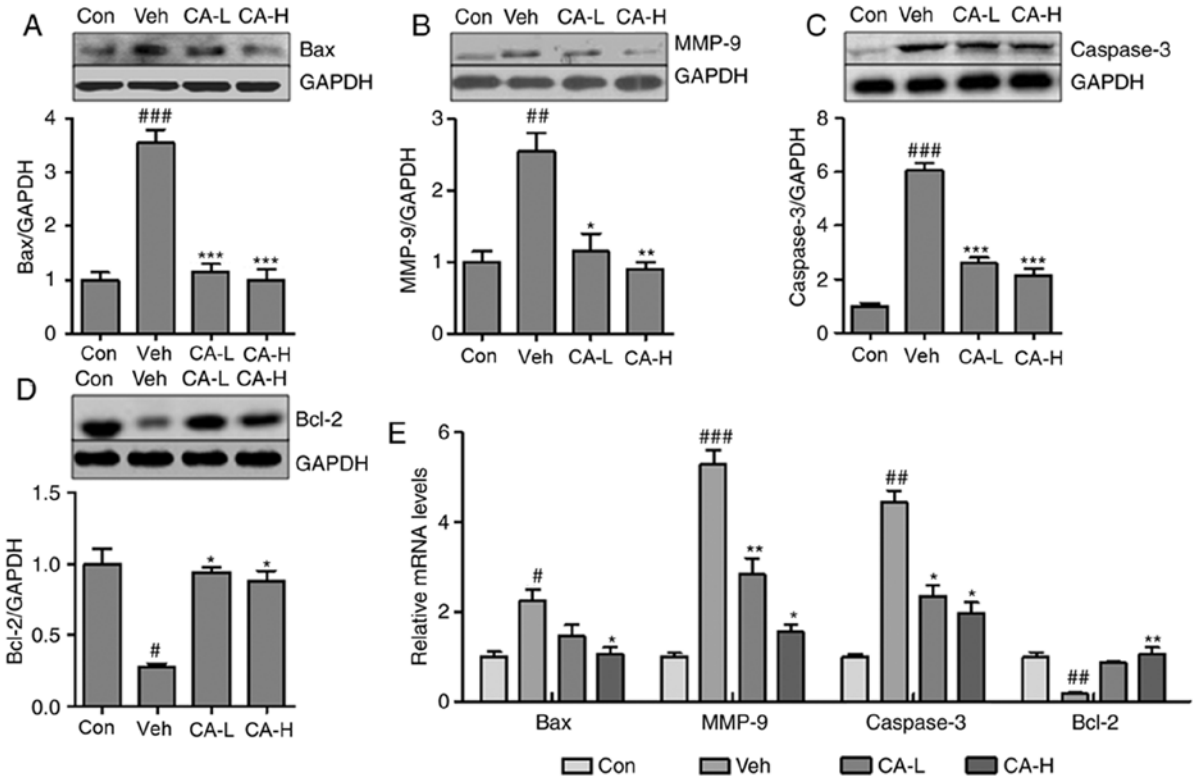

Figure 5. CA alleviates brain injury by suppressing Caspase-3-mediated apoptosis in HFD mice. Protein expression levels of (A) Bax, (B) MMP-9, (C) Caspase-3 and (D) Bcl-2 in the brain of HFD mice, as assessed by western blotting. (E) mRNA expression levels of apoptotic factors in the brain of HFD mice. Data are expressed as the means ± SEM. n=10 in each group. $^{\#}$P<0.05, $^{\#\#}$P<0.01 and $^{\#\#\#}$P<0.001 vs. Con; *P<0.05, **P<0.01 and ***P<0.001 vs. Veh. CA, carnosic acid; CA-H, HFD mice treated with 20 mg/kg CA; CA-L, HFD mice treated with 10 mg/kg CA; Con, Control group; GFAP, glial fibrillary acidic protein; HFD, high-fat diet; MMP-9, matrix metallopeptidase 9; Veh, HFD mice.

levels of Neu-N were significantly upregulated in the Veh group compared with in the Con group (P<0.001). Collectively, it was suggested that HFD caused nerve injury by activating the NF-κB signaling pathway. In addition, HFD increased the protein expression levels of GFAP, Neu-N and Iba-1. Treatment with CA may attenuate brain injury by decreasing the protein expression levels of GFAP, Neu-N, Iba-1 and p-NF-κB.

CA attenuates brain injury by decreasing caspase-3-associated apoptosis. Neurodegeneration has been suggested to be associated with inflammatory response and cell apoptosis (36). Notably, Caspase-3 is an important regulator of apoptosis (37). In the present study, the Caspase-3 apoptotic pathway was investigated. The pro-apoptotic factors Bax and MMP-9 were significantly upregulated in mouse brain tissues from the Veh group compared with in the Con group (P<0.01; Fig. 5A and B). CA treatment significantly decreased the protein expression levels of both factors (P<0.01). Additionally, the protein expression levels of Caspase-3 were increased in the Veh group, but were reduced following CA treatment (P<0.001; Fig. 5C). By contrast, Bcl-2, an anti-apoptotic factor, was significantly downregulated in the Veh group compared with in the Con group (P<0.05), and treatment with CA was sufficient to upregulate the protein expression of Bcl-2 in mouse brain (P<0.05; Fig. 5D). In order to further investigate the expression levels of these factors, RT-qPCR was performed to examine the mRNA expression levels of Bax, MMP-9, Caspase-3 and Bcl-2 in different groups. The qPCR results were consistent with the aforementioned protein expression results (Fig. 5E). Collectively, the present results suggested that CA attenuated nerve injury caused by apoptosis in the mouse brain.

Discussion

A previous study suggested that the incidence of metabolic syndrome is increasing (38). Diabetes is one of the most common metabolic diseases that lead to neurodegeneration (39). The mechanisms underlying neurodegeneration caused by metabolic disease remain unclear. Various therapeutic strategies have been used to treat patients with brain injury caused by metabolic disorders (40). In the present study, the functions of CA, an antioxidant compound extracted from *Rosmarinus officinalis* L., were investigated in a mouse model of HFD-induced metabolic syndrome (16). Previous studies have reported that CA exhibits anti-cancer effects on colon cancer, acute myeloid leukemia and skin cancer by serving as an anti-inflammatory, antioxidant and antimicrobial agent (41-43). However, the molecular mechanisms underlying the effects of CA, which has previously been reported to alleviate brain injury, remain poorly understood (44). Therefore, in the present study, CA was used to investigate the molecular mechanisms regulating neurodegeneration, inflammation and apoptosis.

In the present study, HFD was found to cause metabolic syndrome in mice, which exhibited higher body and liver weights following HFD compared with in the Con group. The present results are in line with a previous study (45). However, body weight and liver weight were significantly decreased following CA administration. Moreover, high serum levels of TG and TC were induced in mice fed a HFD. In the present study, CA was identified as a positive regulator of lipid metabolism, being able to decrease the serum levels of TG and TC. The present results suggested that CA may hold the potential to treat metabolic diseases. In addition, HFD caused an increase in the serum levels of insulin and glucose, and these effects were reversed by CA treatment. The present results suggested that treatment with CA was able to attenuate the deleterious effects of HFD-induced metabolic syndrome.

Metabolic diseases are the primary cause of metabolic-associated inflammation, which is associated with brain injury (46). In the present study, systematic inflammation caused by HFD increased the serum levels of IL-β, IL-6 and TNF-α. In addition, the upregulation of pro-inflammatory cytokines was observed in liver tissue. Notably, treatment with CA downregulated the secretion of pro-inflammatory cytokines in serum and tissue samples. The present results suggested that CA was able to inhibit the inflammatory response, in line with a previous study (20). The NF-κB signaling pathway is involved in the inflammatory response via p-IKKα and p-IκBα (47,48). IKKα is regulated by the ubiquitination and degradation of IκBα, which is mediated by the phosphorylation of this factor. Upon degradation of IκBα, NF-κB can translocate into the nucleus and bind to the κB sites, acting as a transcription factor and promoting the transcription of its downstream genes. In addition, the nuclear translocation of NF-κB can promote the secretion of pro-inflammatory cytokines involved in tissue injury (49). In the present study, the protein expression levels of IL-β, IL-6 and TNF-α in the brain of HFD mice were higher than the Con group, suggesting that activation of the inflammatory response may result in nerve injury. Notably, CA treatment was sufficient to significantly reduce the expression levels of multiple cytokines in the mouse brain. In addition, the protein expression levels of multiple regulators of astrocyte and microglia cell activation (50,51), including GFAP, Iba-1 and Neu-N, were examined by western blot analysis. The protein expression levels of these three factors are associated with the inflammatory response, and GFAP, Iba-1 and Neu-N are biomarkers of central nervous system injury (52). The present results suggested that CA served multiple roles in a mouse model of metabolic syndrome, mediating inactivation of the NF-κB signaling pathway, downregulating the secretion of pro-inflammatory cytokines, and decreasing the expression levels of GFAP, Iba-1 and Neu-N, leading to a reduction in the inflammatory response and an attenuation of brain injury.

A previous study demonstrated that apoptosis-induced cell death is associated with brain injury (53). In the present study, western blot analysis was performed to analyze the Caspase-3 signaling pathway, which is associated with apoptosis (54). Additionally, the protein expression levels of multiple pro-apoptotic factors, including Bax and MMP-9 (55), were investigated. The present results suggested that CA decreased the protein expression levels of Bax and MMP-9 in mouse brain. Similarly, the protein expression levels of Caspase-3 were downregulated. By contrast, the protein expression levels of Bcl-2 were upregulated following CA administration. Therefore, the present results suggested that CA could reduce brain injury by inhibiting apoptosis via the Caspase-3 signal pathway.

In conclusion, HFD induced metabolic syndrome and activated the inflammatory response. Additionally, CA was identified

to regulate lipid metabolism. Moreover, CA alleviated brain injury by decreasing inflammation and apoptosis through the NF-κB and Caspase-3 signaling pathways, respectively. Collectively, the present data suggested that CA may facilitate the development of novel therapies aimed to treat metabolic syndrome.

Acknowledgements

Not applicable.

Funding

The present study was funded by The Natural Science Foundation of Xinjiang Uygur Autonomous Region, China (grant no. 2016D01C152).

Availability of data and materials

The datasets used and/or analyzed during the current study are available from the corresponding author on reasonable request.

Authors' contributions

YoL and YZ designed and performed the experiments, and drafted the manuscript. MH, YuL, YZ, and XC analyzed the data. All authors read and approved the final manuscript.

Ethics approval and consent to participate

The animal experiments were approved by The Committee on The Ethics of Animal Experiments of Xinjiang Medical University (approval no. XM2017MD).

Patient consent for publication

Not applicable.

Competing interests

The authors declare that they have no competing interests.

References

1. Anandhan A, Essa MM and Manivasagam T: Therapeutic attenuation of neuroinflammation and apoptosis by black tea theaflavin in chronic MPTP/probenecid model of Parkinson's disease. Neurotox Res 23: 166-173, 2013.
2. Barnum CJ and Tansey MG: Neuroinflammation and non-motor symptoms: The dark passenger of Parkinson's disease? Curr Neurol Neurosci Rep 12: 350-358, 2012.
3. Khan MM, Kempuraj D, Thangavel R and Zaheer A: Protection of MPTP-induced neuroinflammation and neurodegeneration by Pycnogenol. Neurochem Int 62: 379-388, 2013.
4. Obermeier B, Verma A and Ransohoff RM: The blood-brain barrier. Handb Clin Neurol 133: 39-59, 2016.
5. Fatima G, Das SK and Mahdi AA: Oxidative stress and anti-oxidative parameters and metal ion content in patients with fibromyalgia syndrome: Implications in the pathogenesis of the disease. Clin Exp Rheumatol 31 (6 Suppl 79): S128-S133, 2013.
6. Ghosh A, Kanthasamy A, Joseph J, Anantharam V, Srivastava P, Dranka BP, Kalyanaraman B and Kanthasamy AG: Anti-inflammatory and neuroprotective effects of an orally active apocynin derivative in pre-clinical models of Parkinson's disease. J Neuroinflammation 9: 241, 2012.
7. Yan J, Xu Y, Zhu C, Zhang L, Wu A, Yang Y, Xiong Z, Deng C, Huang XF, Yenari MA, *et al*: Simvastatin prevents dopaminergic neurodegeneration in experimental parkinsonian models: The association with anti-inflammatory responses. PLoS One 6: e20945, 2011.
8. Chen WW, Zhang X and Huang WJ: Role of neuroinflammation in neurodegenerative diseases (Review). Mol Med Rep 13: 3391-3396, 2016.
9. Nizamutdinov D and Shapiro LA: Overview of traumatic brain injury: An immunological context. Brain Sci 7: E11, 2017.
10. Mukandala G, Tynan R, Lanigan S and O'Connor JJ: The effects of hypoxia and inflammation on synaptic signaling in the CNS. Brain Sci 6: E6, 2016.
11. Ghosh A, Birngruber T, Sattler W, Kroath T, Ratzer M, Sinner F and Pieber TR: Assessment of blood-brain barrier function and the neuroinflammatory response in the rat brain by using cerebral open flow microperfusion (cOFM). PLoS One 9: e98143, 2014.
12. Czabotar PE, Lessene G, Strasser A and Adams JM: Control of apoptosis by the BCL-2 protein family: Implications for physiology and therapy. Nat Rev Mol Cell Biol 15: 49-63, 2014.
13. Koff JL, Ramachandiran S and Bernal-Mizrachi L: A time to kill: Targeting apoptosis in cancer. Int J Mol Sci 16: 2942-2955, 2015.
14. Rajan TS, Giacoppo S, Trubiani O, Diomede F, Piattelli A, Bramanti P and Mazzon E: Conditioned medium of periodontal ligament mesenchymal stem cells exert anti-inflammatory effects in lipopolysaccharide-activated mouse motoneurons. Exp Cell Res 349: 152-161, 2016.
15. Mengoni ES, Vichera G, Rigano LA, Rodriguez Puebla ML, Galliano SR, Cafferata EE, Pivetta OH, Moreno S and Vojnov AA: Suppression of COX-2, IL-1β and TNF-α expression and leukocyte infiltration in inflamed skin by bioactive compounds from *Rosmarinus officinalis* L. Fitoterapia 8: 414-421, 2011.
16. Moore J, Yousef M and Tsiani E: Anticancer effects of rosemary (*Rosmarinus officinalis* L.) extract and rosemary extract polyphenols. Nutrients 8: E731, 2016.
17. Jung KJ, Min KJ, Bae JH and Kwon TK: Carnosic acid sensitized TRAIL-mediated apoptosis through down-regulation of c-FLIP and Bcl-2 expression at the post translational levels and CHOP-dependent up-regulation of DR5, Bim, and PUMA expression in human carcinoma caki cells. Oncotarget 6: 1556-1568, 2015.
18. Tamaki Y, Tabuchi T, Takahashi T, Kosaka K and Satoh T: Activated glutathione metabolism participates in protective effects of carnosic acid against oxidative stress in neuronal HT22 cells. Planta Medica 76: 683-688, 2010.
19. Tsai CW, Liu KL, Lin YR and Kuo WC: The mechanisms of carnosic acid attenuates tumor necrosis factor-α-mediated inflammation and insulin resistance in 3T3-L1 adipocytes. Mol Nutr Food Res 58: 654-664, 2014.
20. Oh J, Yu T, Choi SJ, Yang Y, Baek HS, An SA, Kwon LK, Kim J, Rho HS, Shin SS, *et al*: Syk/Src pathway-targeted inhibition of skin inflammatory responses by carnosic acid. Mediators Inflamm 2012: 781375, 2012.
21. Meng P, Yoshida H, Matsumiya T, Imaizumi T, Tanji K, Xing F, Hayakari R, Dempoya J, Tatsuta T, Aizawa-Yashiro T, *et al*: Carnosic acid suppresses the production of amyloid-β 1-42 by inducing the metalloprotease gene TACE/ADAM17 in SH-SY5Y human neuroblastoma cells. Neurosci Res 75: 94-102, 2013.
22. Chen JH, Ou HP, Lin CY, Lin FJ, Wu CR, Chang SW and Tsai CW: Carnosic acid prevents 6-hydroxydopamine-induced cell death in SH-SY5Y cells via mediation of glutathione synthesis. Chem Res Toxicol 25: 1893-1901, 2012.
23. National Research Council (US) Committee for the Update of the Guide for the Care and Use of Laboratory Animals: Guide for the Care and Use of Laboratory Animals. 8th edition. National Academies Press (US), Washington, DC, 2011.
24. Zhao Y, Sedighi R, Wang P, Chen H, Zhu Y and Sang S: Carnosic acid as a major bioactive component in rosemary extract ameliorates high-fat-diet-induced obesity and metabolic syndrome in mice. J Agric Food Chem 63: 4843-4852, 2015.
25. Alberti KG and Zimmet PZ: Definition, diagnosis and classification of diabetes mellitus and its complications. Part 1: Diagnosis and classification of diabetes mellitus provisional report of a WHO consultation. Diabet Med 15: 539-553, 1998.
26. Chan JK: The wonderful colors of the hematoxylin-eosin stain in diagnostic surgical pathology. Int J Surg Pathol 22: 12-32, 2014.
27. Gouze E, Pawliuk R, Gouze JN, Pilapil C, Fleet C, Palmer GD, Evans CH, Leboulch P and Ghivizzani SC: Lentiviral-mediated gene delivery to synovium: Potent intra-articular expression with amplification by inflammation. Mol Ther 7: 460-466, 2003.

28. Kramer AS, Latham B, Diepeveen LA, Mou L, Laurent GJ, Elsegood C, Ochoa-Callejero L and Yeoh GC: InForm software: A semi-automated research tool to identify presumptive human hepatic progenitor cells, and other histological features of pathological significance. Sci Rep 8: 3418, 2018.
29. Livak KJ and Schmittgen TD: Analysis of relative gene expression data using real-time quantitative PCR and the 2(-Delta Delta C(T)) method. Methods 25: 402-408, 2001.
30. Yu W, Wu J, Cai F, Xiang J, Zha W, Fan D, Guo S, Ming Z and Liu C: Curcumin alleviates diabetic cardiomyopathy in experimental diabetic rats. PLoS One 7: e520132012, 2012.
31. Klöting N and Blüher M: Adipocyte dysfunction, inflammation and metabolic syndrome. Rev Nedcor Metab Disord 15: 277-287, 2014.
32. Pozniak PD, White MK and Khalili K: TNF-α/NF-κB signaling in the CNS: Possible connection to EPHB2. J Neuroimmune Pharmacol 9: 133-141, 2014.
33. Ricci G, Pirillo I, Tomassoni D, Sirignano A and Grappasonni I: Metabolic syndrome, hypertension, and nervous system injury: Epidemiological correlates. Clin Exp Hypertens 39: 8-16, 2017.
34. Wan F and Lenardo MJ: The nuclear signaling of NF-kappaB: Current knowledge, new insights, and future perspectives. Cell Res 20: 24-33, 2010.
35. Bramanti V, Tomassoni D, Avitabile M, Amenta F and Avola R: Biomarkers of glial cell proliferation and differentiation in culture. Front Biosci (Schol Ed) 2: 558-570, 2010.
36. Shalini S, Dorstyn L, Dawar S and Kumar S: Old, new and emerging functions of caspases. Cell Death Differ 22: 526-539, 2015.
37. D'Amelio M, Sheng M and Cecconi F: Caspase-3 in the central nervous system: Beyond apoptosis. Trends Neurosci 35: 700-709, 2012.
38. Kaur J: A comprehensive review on metabolic syndrome. Cardiol Res Pract 2014: 943162, 2014.
39. Bartzokis G: Alzheimer's disease as homeostatic responses to age-related myelin breakdown. Neurobiol Aging 32: 1341-1371, 2011.
40. He Q, Liu J, Liang J, Liu X, Li W, Liu Z, Ding Z and Tuo D: Towards improvements for penetrating the blood-brain barrier-recent progress from a material and pharmaceutical perspective. Cells 7: E24, 2018.
41. Barni MV, Carlini MJ, Cafferata EG, Puricelli L and Moreno S: Carnosic acid inhibits the proliferation and migration capacity of human colorectal cancer cells. Oncol Rep 27: 1041-1048, 2012.
42. Pesakhov S, Khanin M, Studzinski GP and Danilenko M: Distinct combinatorial effects of the plant polyphenols curcumin, carnosic acid, and silibinin on proliferation and apoptosis in acute myeloid leukemia cells. Nutr Cancer 62: 811-824, 2010.
43. Park M, Han J, Lee CS, Soo BH, Lim KM and Ha H: Carnosic acid, a phenolic diterpene from rosemary, prevents UV-induced expression of matrix metalloproteinases in human skin fibroblasts and keratinocytes. Exp Dermatol 22: 336-341, 2013.
44. Maynard ME, Underwood EL, Redell JB, Zhao J, Kobori N, Hood KN, Moore AN and Dash PK: Carnosic acid improves outcome after repetitive mild traumatic brain injury. J Neurotrauma: Mar 26, 2019 (Epub ahead of print).
45. Lee YS, Cha BY, Saito K, Choi SS, Wang XX, Choi BK, Yonezawa T, Teruya T, Nagai K and Woo JT: Effects of a Citrus depressa Hayata (shiikuwavsa) extract on obesity in high-fat diet-induced obese mice. Phytomedicine 18: 648-654, 2011.
46. Karelina K and Weil ZM: Neuroenergetics of traumatic brain injury. Concussion 1: CNC9, 2015.
47. Cao C, Zhu Y, Chen W, Li L, Qi Y, Wang X, Zhao Y, Wan X and Chen X: IKKε knockout prevents high fat diet induced arterial atherosclerosis and NF-κB signaling in mice. PLoS One 8: e64930, 2013.
48. Verhelst K, Verstrepen L, Carpentier I and Beyaert R: IκB kinase ε (IKKε): A therapeutic target in inflammation and cancer. Biochem Pharmacol 85: 873-880, 2013.
49. Liu T, Zhang L, Joo D and Sun SC: NF-κB signaling in inflammation. Signal Transduct Target Ther 2: 17023, 2017.
50. Simpson JE, Ince PG, Lace G, Forster G, Shaw PJ, Matthews F, Savva G, Brayne C and Wharton SB; MRC Cognitive Function and Ageing Neuropathology Study Group: Astrocyte phenotype in relation to Alzheimer-type pathology in the ageing brain. Neurobiol Aging 31: 578-590, 2010.
51. Tremblay ME, Zettel ML, Ison JR, Allen PD and Majewska AK: Effects of aging and sensory loss on glial cells in mouse visual and auditory cortices. Glia 60: 541-558, 2012.
52. Lyck L, Dalmau I, Chemnitz J, Finsen B and Schrøder HD: Immunohistochemical markers for quantitative studies of neurons and glia in human neocortex. J Histochem Cytochem 56: 201-221, 2008.
53. Zlatic S, Comstra HS, Gokhale A, Petris MJ and Faundez V: Molecular basis of neurodegeneration and neurodevelopmental defects in Menkes disease. Neurobiol Dis 81: 154-161, 2015.
54. Simon DJ, Weimer RM, McLaughlin T, Kallop D, Stanger K, Yang J, O'Leary DD, Hannoush RN and Tessier-Lavigne M: A caspase cascade regulating developmental axon degeneration. J Neurosci 32: 17540-17553, 2012.
55. Olsson M and Zhivotovsky B: Caspases and cancer. Cell Death Differ 18: 1441-1449, 2011.